AIAA JOURNAL
Vol. 40, No. 6, June 2002

Piezoelectric Sensor and Actuator Spatial Design for Shape Control of Piezolaminated Plates

Abhijit Mukherjee* and Shailendra Joshi†
Indian Institute of Technology Bombay, Mumbai 400 076, India

Controlled actuation and sensing of structures by spatially distributing the piezoelectric material has been a topic of interest in recent years. We present an iterative technique to design the shape of piezoelectric actuators in order to achieve the desired shape of the structure. A gradientless shape design procedure based on the residual voltages is developed. It aims at minimizing the quadratic measure of global displacement residual error between the desired and the current structural configuration. The actuators gradually adapt to a shape that is most efficient in resisting the external excitation. The present technique can be well suited for any static and time-varying excitation. In vibration control it is often necessary to create modal sensors and actuators in order to observe or excite some specific modes. Such modal sensors and actuators alleviate spillover problems, and thus they avoid exhaustive signal processing. Several numerical examples for static as well as dynamic cases are presented to demonstrate the efficacy of the present technique.

Nomenclature

$\boldsymbol{B}$	=	strain-displacement matrix
C	=	capacitance of the piezoelectric material
$\boldsymbol{D}$	=	dielectric displacement vector
$\boldsymbol{E}$	=	electric field vector
$\boldsymbol{e}$	=	matrix of piezoelectric stress constants
$\boldsymbol{N}^p, \boldsymbol{M}^p$	=	actuator force and moment resultants
$\boldsymbol{Q}$	=	matrix of elastic constants
q	=	closed-circuit charge
V_S	=	sensor voltage
α	=	quadratic measure of residual error between desired shape and actual shape
$\boldsymbol{\delta}_e$	=	nodal displacement vector
$\bar{\epsilon}$	=	matrix of dielectric constants
$\boldsymbol{\varepsilon}$	=	mechanical strain vector
$\boldsymbol{\sigma}$	=	stress vector induced by mechanical and electrical effects

I. Introduction

PIEZOELECTRIC materials are widely used in the development of high-performance structures that are energy efficient and autonomous, known as *smart structures*. These materials are capable of sensing and controlling the changes in the structural characteristics. Optimal distribution of the piezoelectric material in the structure to induce controlled actuation has been a subject of interest in recent years. In many practical situations (for example, reflector antennas, deformable mirrors, aircraft wings, etc.) this is of utmost importance in order to exercise precise control over the shape of the structure. In dynamic conditions it is often desirable to observe or excite specific modes of interest. Optimal spatial distribution of piezoelectric material allows observation or excitation of desired modes without exhaustive signal processing. In this paper we demonstrate a technique for optimum shape design of sensors and actuators in controlling plate structures.

Some reviews on controlled actuation are available.[1,2] Several research works have been carried out on developing techniques for the placement of discrete number of actuators to control the response of the structure. Lim[3] proposed a method of determining the optimal subset of actuators and sensors based on a weighted measure of modal participation of each sensor/actuator combination. Gawronski and Lim[4] employed a placement index based on the Hankel singular values (HSV) to determine the sensor and actuator locations that maximize observability and controllability criteria. Clark and Cox[5] experimentally demonstrated a band-limited method based on HSV decomposition for selecting actuators and sensors to filter out the modes outside the desired bandwidth for structural acoustic control. Gaudenzi and Barboni[6] determined the size and location of the discrete actuators for Euler–Bernoulli beams by applying a number of constraints that uniquely define the design variables. However, this method requires artificial constraints to generate unique solutions. Barboni et al.[7] employed the pin-force model and the modal approach to obtain closed-form solutions for optimal size and location of actuators on beams under dynamic conditions. Seeley and Chattopadhyay[8] solved a multiobjective optimization problem that includes discrete actuator location, vibration reduction, reduction in power consumption, and maximization of fundamental frequency in the objective function. A nonlinear constrained programming approach based on the method of feasible directions was employed in the solution of cantilever box beams. Kapania et al.[9] used a heuristic integer programming approach to determine optimal locations of actuators in the control of thermal deformations of spherical mirror segments. Onoda and Hanawa[10] used genetic algorithms (GA) and simulated annealing algorithms for optimal placement of actuators in shape control of space trusses. Zhang et al.[11] employed a GA for sensor and actuator locations and the feedback gains simultaneously. Kang et al.[12] presented a gradient-based numerical scheme based on the damping characteristics to optimize the sensor and actuator placement for vibration control of plates.

Some investigators have used optimal voltage distribution in the control of the structures. Lin and Hsu[13] used sine-shaped sensors in the static control of beams. The voltage distribution in sensors and actuators are written in terms of the displacements, and the solution is obtained using Fourier sine series. Agrawal and Treanor[14] presented analytical and experimental results on optimal placement of actuators and optimal voltages for beams. They developed an algorithm that optimized actuator placement and voltages for a given shape function. The authors reported that simultaneous optimization of actuator position and input voltages were unreliable because of the differences in the order of actuator locations and voltage terms in the optimization of cost function. Soares et al.[2] used gradient-based optimization techniques for optimal design of piezolaminated structures. In the static shape control of plates, the voltages were found by minimizing the mean-squared error between the desired and actual

Received 19 May 2001; revision received 2 October 2001; accepted for publication 19 November 2001.

*Professor, Department of Civil Engineering.
†Research Student, Department of Civil Engineering.

transverse displacements. In practice, the control of structures using distributed voltage requires electrical circuitry that might involve complexities and loss of signal as a result of leakages in the electrical connections. Moreover, the techniques are limited to actuation and cannot be employed in sensing.

An alternative to the just-mentioned methods is to distribute the piezoelectric material over the structure surface. This involves shaping the material and selectively polarizing it to obtain the desired response. The range of wavelengths over which discrete transducers function properly is limited by spatial aliasing. However, continuously distributed transducers have no such limitation, as spatial aliasing does not occur. Further, because of variable transducer weighting in terms of geometry and material polarization less signal processing is required. Lee and Moon[15] developed a theory to derive modal sensors and actuators for one-dimensional structures using modal equations. They conducted experiments on a cantilever beam by fabricating mode 1 and mode 2 sensors. These modal sensors and actuators overcome spillover problems. However, the theory is difficult to apply to the structures with complex boundary conditions, as the closed-form solutions might not be available. Collins et al.[16] presented a design technique based on the traveling wave characteristics of the structural deformations to design the spatial weighting of transducers to produce spatial filters. Friswell[17] used finite element shape functions to determine the sensor and actuator shapes for Euler–Bernoulli beams. Gaudenzi et al.[18] demonstrated the use of GA in determining actuator distribution for beams. Ryou et al.[19] employed GA in designing the electrode patterns of piezoelectric sensors and actuators. Mukherjee and Joshi[20] presented an iterative design procedure for determining actuator profiles for minimum power consumption in achieving specified displacements in plates. Clark and Burke[21] highlighted the limitations on achieving shaped modal sensors. Their analytical and experimental investigations showed that a small error in the placement of a modal sensor gives rise to contributions from undesired modes.

The present work deals with developing spatially continuous transducers to achieve desired structural control. It can be seen from the preceding discussion that most attempts at optimal sensing and actuation have been for beam and truss-type structures that are devoid of complicating effects such as torsional excitation, inplane-transverse coupling, and small aspect ratios. In such structures it is possible to intuitively design the shape of the actuators and sensors that is very close to optimum. In presence of the complicating effects just mentioned, an intuitive design is far more difficult, if not impossible. The present paper demonstrates a technique for the adaptive shape design of actuator and sensor profiles that is able to accommodate the complexities in structural configurations and excitation. A gradientless procedure based on the residual voltages is developed. It aims at minimizing the quadratic measure of global displacement residual error between the desired and the current structural configuration. The actuators gradually adapt to a shape that is most efficient in controlling the structure. The importance of anisotropic actuation has been highlighted for structures that have smaller aspect ratios or coupled mode problems.

In dynamic conditions it is desirable to minimize spillover effect during structural control. The present technique has been used in determining sensor or actuator profiles that respond primarily to the desired modes while diminishing the contribution from the other modes. The efficacy of the designed shapes has been far superior to the conventional designs.

II. Mathematical Model

A. Piezoelectric Constitutive Relations

The linear constitutive relations for a kth layer of a laminated plate bonded with piezoelectric layers are given as

$$\boldsymbol{\sigma}^k = (\boldsymbol{Q}\boldsymbol{\epsilon} - \boldsymbol{e}^t\boldsymbol{E})^k \tag{1}$$

$$\boldsymbol{D}^k = (\boldsymbol{e}\boldsymbol{\epsilon} + \bar{\boldsymbol{\epsilon}}\boldsymbol{E})^k \tag{2}$$

Equations (1) and (2) are called as the direct and the converse piezoelectric effects, respectively, as they couple electrical energy with mechanical energy. If the piezoelectric effects are absent, Eq. (1) is reduced to the stress-strain relation of a conventional elastic body.

B. Displacement Field

The displacement field of a laminated plate based on the first-order shear-deformation theory is given by

$$\begin{aligned} U(x, y, z, t) &= u_0 - z\theta_y(x, y, t) \\ V(x, y, z, t) &= v_0 + z\theta_x(x, y, t) \\ W(x, y, z, t) &= w_0(x, y, t) \end{aligned} \tag{3}$$

The terms u_0, v_0, and w_0 are the midplane displacements, and θ_x and θ_y are the rotations of transverse normal about x and y axes. Using isoparametric relationships, the coordinates and displacements inside the element are defined as

$$x = \sum_{i=1}^{n} N_i x_i, \qquad y = \sum_{i=1}^{n} N_i y_i, \qquad u = \sum_{i=1}^{n} N_i \delta_i \tag{4}$$

where N_i are the element shape functions and n is the number of nodes per element. In the present work an eight-node C^0-continuous plate element is employed in the analysis of piezolaminated plates.

C. Strain-Displacement Relation

The strain components at any point along the thickness of the plate are written in terms of strains at the reference plane as

$$\boldsymbol{\epsilon} = \begin{Bmatrix} \varepsilon_x \\ \varepsilon_y \\ \gamma_{xy} \\ \gamma_{yz} \\ \gamma_{xz} \end{Bmatrix} = \begin{Bmatrix} \dfrac{\partial U}{\partial x} \\ \dfrac{\partial V}{\partial y} \\ \dfrac{\partial U}{\partial x} + \dfrac{\partial V}{\partial x} \\ \dfrac{\partial W}{\partial y} + \theta_x \\ \dfrac{\partial W}{\partial x} - \theta_y \end{Bmatrix}$$

$$= \begin{Bmatrix} \left(\dfrac{\partial u_0}{\partial x} - z\dfrac{\partial \theta_y}{\partial x}\right) \\ \left(\dfrac{\partial v_0}{\partial y} + z\dfrac{\partial \theta_x}{\partial y}\right) \\ \left(\dfrac{\partial u_0}{\partial y} - z\dfrac{\partial \theta_y}{\partial y}\right) + \left(\dfrac{\partial v_0}{\partial x} + z\dfrac{\partial \theta_x}{\partial x}\right) \\ \left(\dfrac{\partial w_0}{\partial y} + \theta_x\right) \\ \left(\dfrac{\partial w_0}{\partial y} - \theta_y\right) \end{Bmatrix} \tag{5}$$

Equation (5) can be written in concise form as

$$\boldsymbol{\epsilon} = \boldsymbol{H}\bar{\boldsymbol{\epsilon}} \tag{6}$$

where

$$\bar{\epsilon}^t = \left[\frac{\partial u_0}{\partial x}, \frac{\partial v_0}{\partial y}, \left(\frac{\partial u_0}{\partial y} + \frac{\partial v_0}{\partial x}\right), \frac{\partial \theta_x}{\partial y}, -\frac{\partial \theta_y}{\partial x}, \left(\frac{\partial \theta_x}{\partial x} - \frac{\partial \theta_y}{\partial y}\right)\left(\frac{\partial w}{\partial x} - \theta_y\right), \left(\frac{\partial w}{\partial y} - \theta_x\right)\right] \tag{7}$$

$$\boldsymbol{H} = \begin{bmatrix} 1 & 0 & 0 & 0 & z & 0 & 0 & 0 \\ 0 & 1 & 0 & z & 0 & 0 & 0 & 0 \\ 0 & 0 & 1 & 0 & 0 & z & 0 & 0 \\ 0 & 0 & 0 & 0 & 0 & 0 & 1 & 0 \\ 0 & 0 & 0 & 0 & 0 & 0 & 0 & 1 \end{bmatrix} \tag{8}$$

The strains at the reference plane are related to the nodal displacements via strain-displacement matrix as follows:

$$\bar{\epsilon} = \boldsymbol{B}\boldsymbol{\delta}_e \tag{9}$$

where

$$\boldsymbol{\delta}_e = (u_0, v_0, w_0, \theta_x, \theta_y)^t \tag{10}$$

$$\boldsymbol{B} = \sum_{r=1}^{n} \begin{bmatrix} \frac{\partial N_r}{\partial x} & 0 & 0 & 0 & 0 \\ 0 & \frac{\partial N_r}{\partial y} & 0 & 0 & 0 \\ \frac{\partial N_r}{\partial y} & \frac{\partial N_r}{\partial x} & 0 & 0 & 0 \\ 0 & 0 & 0 & \frac{\partial N_r}{\partial y} & 0 \\ 0 & 0 & 0 & 0 & -\frac{\partial N_r}{\partial x} \\ 0 & 0 & 0 & \frac{\partial N_r}{\partial x} & -\frac{\partial N_r}{\partial y} \\ 0 & 0 & \frac{\partial N_r}{\partial y} & N_r & 0 \\ 0 & 0 & \frac{\partial N_r}{\partial x} & 0 & -N_r \end{bmatrix} \tag{11}$$

D. Stress-Strain Relation

The laminated piezoelectric plate equations are obtained by integrating Eq. (1) through the thickness:

$$\begin{Bmatrix} \boldsymbol{N} \\ \boldsymbol{M} \end{Bmatrix} = \bar{\boldsymbol{D}} \begin{Bmatrix} \varepsilon \\ \kappa \end{Bmatrix} - \begin{Bmatrix} \boldsymbol{N}^P \\ \boldsymbol{M}^P \end{Bmatrix}, \qquad \begin{Bmatrix} \boldsymbol{Q}_x \\ \boldsymbol{Q}_y \end{Bmatrix} = \begin{bmatrix} \boldsymbol{S}_{44} & \boldsymbol{S}_{45} \\ \boldsymbol{S}_{54} & \boldsymbol{S}_{55} \end{bmatrix} \begin{Bmatrix} \gamma_{xz} \\ \gamma_{yz} \end{Bmatrix} \tag{12}$$

where

$$\bar{\boldsymbol{D}} = \int \boldsymbol{H}^t \boldsymbol{Q} \boldsymbol{H}\, \mathrm{d}z \tag{13}$$

$\boldsymbol{Q}_x$ and $\boldsymbol{Q}_y$ are the shear-stress resultants. The piezoelectric stress resultants are derived in the following section.

III. Actuator and Sensor Mechanics

If the voltage is applied to the piezoelectric layer only in the thickness direction, the electric field intensity $(E_3)^k$ in the equation is expressed as

$$(E_3)^k = V^k / h^k \tag{14}$$

where V^k is the applied voltage across kth layer and h^k is the thickness of kth layer. The actuator force and moment resultants written in Eq. (12) are given as

$$\begin{Bmatrix} \boldsymbol{N}_x^P & \boldsymbol{M}_x^P \\ \boldsymbol{N}_y^P & \boldsymbol{M}_y^P \\ \boldsymbol{N}_{xy}^P & \boldsymbol{M}_{xy}^P \end{Bmatrix} = \sum_{k=1}^{N\text{lay}} \int_{z(k-1)}^{z(k)} \begin{Bmatrix} \boldsymbol{e}_{31} \\ \boldsymbol{e}_{32} \\ 0 \end{Bmatrix}^k \{1, z\}(E_3)^k\, \mathrm{d}z \tag{15}$$

The actuator nodal force vector is obtained as

$$\boldsymbol{F}^P = \iint_A \boldsymbol{B}^T \begin{Bmatrix} \boldsymbol{N}^P \\ \boldsymbol{M}^P \end{Bmatrix} \mathrm{d}A \tag{16}$$

According to the Gauss law, the closed-circuit charge q measured through the electrodes of a sensor patch in kth layer is

$$q = \frac{1}{2}\left[\left(\int_R D_3^k\, \mathrm{d}A \right)_{z=z_k} + \left(\int_R D_3^k\, \mathrm{d}A \right)_{z=z_{k-1}} \right] \tag{17}$$

where D_3^k is the dielectric displacement in the 3-direction and R is the effective surface electrode of the patch. Substituting Eqs. (2) and (9) into the preceding equation, we get

$$q = \int_R (\boldsymbol{e}\boldsymbol{B}\boldsymbol{\delta}_e)\, \mathrm{d}A \tag{18}$$

The sensor voltage is computed as

$$V_s = q / C \tag{19}$$

IV. Sensor and Actuator Shape Design

In this section we present the iterative algorithm for adaptive design of sensor and actuator profiles. The present design method can be applied for static as well as dynamic cases. In static analysis the objective is to determine the actuator profile that attempts to obtain the desired shape of the structure after it has deformed under external forces. In dynamic analysis the sensor or the actuator configurations corresponding to the mode shapes that are to be observed or excited are determined. A reciprocal relationship exists between the sensor and the actuator. Therefore, the shape of the sensor that responds to a particular mode (modal sensor) is also the shape of the actuator that excites that mode (modal actuator). The present iterative procedure can therefore be employed in designing both modal sensors and actuators. The objective is to minimize the quadratic measure of the residual deviation of the current deformations of the structure from its desired state. The objective function is thus defined as

$$\text{minimize} \left[\int \{\boldsymbol{\delta}_i(p_1, A_1, \ldots, p_n, A_n) - \boldsymbol{\delta}_0\}^2\, \mathrm{d}A \right] \tag{20}$$

where $\boldsymbol{\delta}_i$ is the normalized deformation vector in ith iteration; $A_i, \ldots, A_n$ are areas of actuators that are switched on; $(p_1, \ldots, p_n)$ is the actuator position vector; and $\boldsymbol{\delta}_0$ is the normalized desired deformation vector.

The step-by-step procedure for the solution is described here:

1) The entire structural domain is discretized using a fine finite element mesh.

2) In case of static analysis, the deformation vector is the solution obtained after analyzing the structure for external mechanical loads. In the dynamic analysis the mode shape for which the sensor/actuator profile is to be obtained is the deformation vector. Using Eq. (19), the voltage in each element (V_s^e) is calculated.

3) The shape design process begins with a maximal seed design in that all actuators are switched on. The process continues toward shape determination by removing the undesired actuators. To begin the process of removal of actuators, a novel concept of front opening is implemented (Fig. 1). The front is defined by the physical boundaries of the structure. The actuators that lie on the front are removed from the locations of minimal absolute curvature. This is termed the *front opening*. The actuators that surround the front are candidates for state change.

4) The structure is analyzed based on the current actuator configuration under unit voltage, and the voltages developed as a result of current actuator configuration are calculated V_a^e.

5) The voltages V_a^e and V_s^e are normalized with respect to their maximum values:

$$\bar{V}_s^e = \frac{V_s^e}{\left(V_s^e\right)_{\max}}, \qquad \bar{V}_a^e = \frac{V_a^e}{\left(V_a^e\right)_{\max}} \tag{21}$$

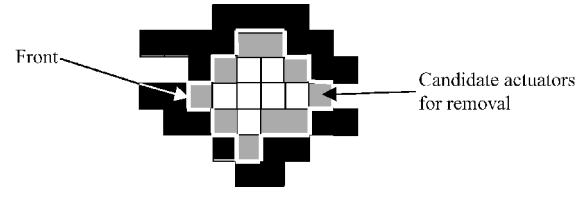

Fig. 1 Front growth.

The residual voltages V_r^e for the elements on the front are determined as

$$V_r^e = \left(\bar{V}_s^e - \bar{V}_a^e\right) \tag{22}$$

The elements that have negative residuals are potential actuators to be removed. In practice, a predetermined fraction of these actuators is removed.

6) The quadratic measure of the global residual deviation α in deformation is calculated as

$$\alpha = \sum_{i=1}^{\text{ndof}} (\delta_i - \delta_0)^2 \tag{23}$$

7) Steps 4–6 are repeated until the value of α is acceptably small.

V. Numerical Results and Discussion

The actuator shape design technique described in the preceding section is validated solving the cases for which solutions can be obtained by hand calculations. Subsequently, several cases with different aspect ratios are analyzed for static and dynamic excitations. Table 1 contains the properties of the plate and the piezoelectric material for all of the examples.

A. Static Analysis

In the first two examples we consider plates with large aspect ratios that can be treated as one-dimensional structures. The actuator profiles for these structures under a given external load can be determined by physical intuition or by hand calculations. Subsequently, plates with smaller aspect ratios are considered to investigate the two-dimensional case. The importance of anisotropic actuation in the control of coupled twist-bending deformations is also highlighted.

Example 1: A cantilever plate subjected to uniform pressure. A long cantilever plate (0.1×0.02 m) made of aluminum is subjected to unit pressure. The objective is to find out the actuator layout that gives the original undeformed shape under the given load. Using symmetric boundary conditions, only half the structure is modeled with a 75×7 finite element (FE) mesh. The piezoelectric effect e_{32} is neglected in order to compare the result with one-dimensional solution. Of the total number of actuators that lie on the front, two actuators that satisfy the condition [Eq. (12)] explained in the design procedure are removed in each iteration. Figures 2a–2d show the actuator configurations at different stages of the design process. The optimal shape for the problem is shown in Fig. 2d. The method produces a design that is very close to the optimal shape. The global error in displacement reduces monotonically until the minimum value is reached (Fig. 3). Beyond this point any further removal leads to increase in the error.

Example 2: A simply supported long plate subjected to uniform pressure. The boundary conditions for the plate in the first example are modified, and the plate is simply supported at two short edges. The plate is subjected to a unit pressure and the actuator profile to regain the original undeformed configuration is determined (Figs. 4a–4c). Like the preceding example, the piezoelectric effect e_{32} is neglected. Figure 5 shows the convergence history of the design.

Table 1 Constituent properties

Property	PVDF	Aluminum	Graphite epoxy
Young's modulus, GPa, E_1, E_2	2.0, 2.0	70.0, 70.0	150.0, 9.0
Poisson's ratio, ν_{12}	0.30	0.25	0.30
Shear modulus, GPa, G_{12}, G_{23}, G_{13}	0.775, 0.775, 0.0775	28.0, 28.0, 28.0	7.1, 2.5, 7.1
Piezoelectric constant, C/m^2, $e_{31} = e_{32}$	−0.046	——	——
Thickness of each layer, mm	0.50	0.50	0.50
Number of layers	2 (each at top and bottom)	2 (between the piezoelectric layers)	3
Mass density, N s/m^4, ρ	1800	2700	1600

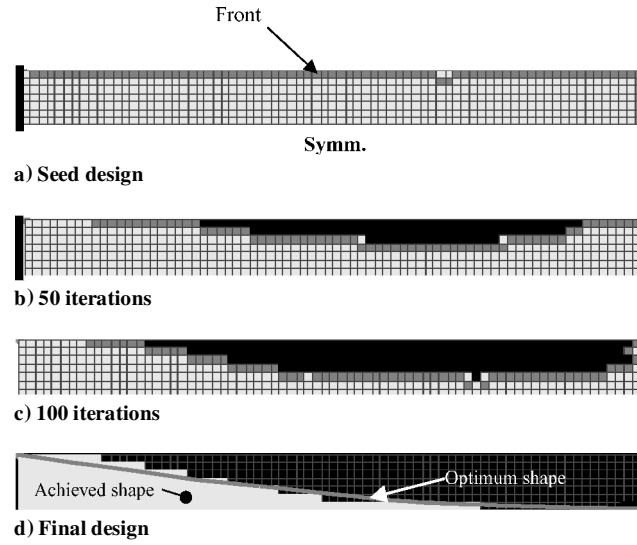

Fig. 2 Actuator design history (example 1).

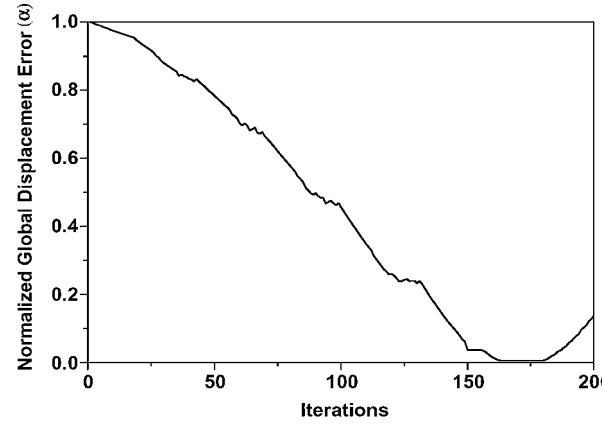

Fig. 3 Error history (example 1).

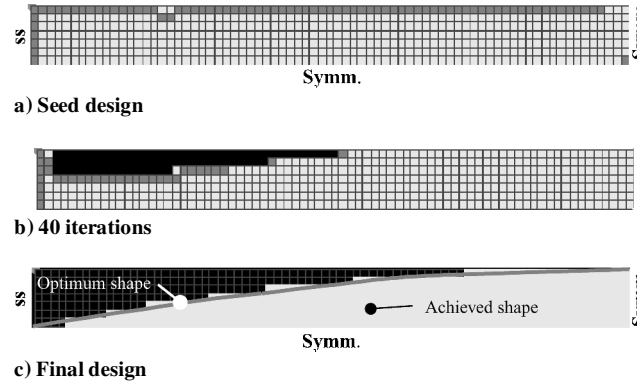

Fig. 4 Actuator design history (example 2).

Example 3: A simply supported rectangular plate subjected to uniform pressure. In the preceding examples plates with large aspect ratio were considered. The piezoelectric effect in the shorter direction was neglected so that the results could be compared to one-dimensional solutions. In this example we consider an aluminum plate with smaller aspect ratio (0.2×0.1 m), simply supported at all four edges. The plate is subjected to uniform unit pressure. The piezoelectric effects in both the directions are important. Four actuators of the possible candidate actuators are removed in each iteration (Figs. 6a–6d). The error curve (Fig. 7) highlights an important aspect of the present design procedure. The solution successfully crosses the local minima and proceeds to reach the global minimum.

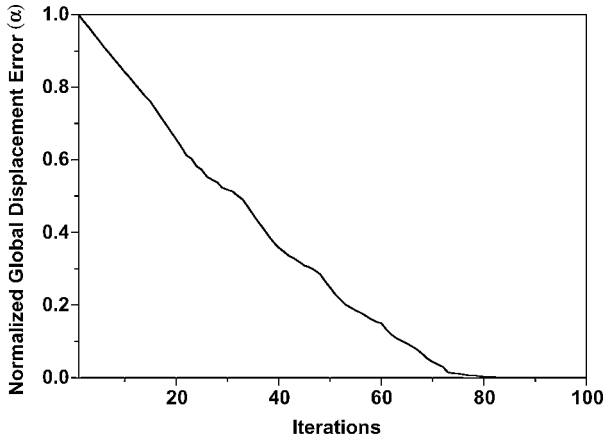

Fig. 5 Error history (example 2).

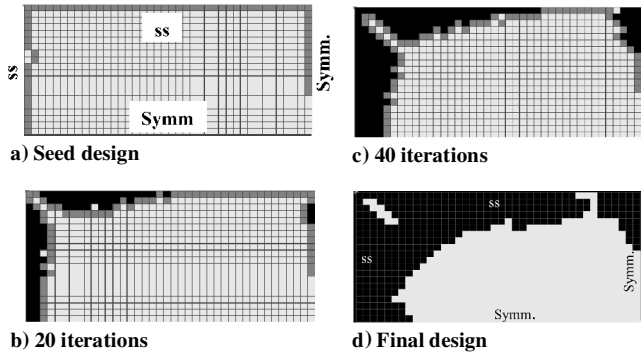

Fig. 6 Actuator design history (example 3).

Fig. 7 Error history (example 3).

Example 4: A cantilever laminated plate under uniform pressure. A graphite-epoxy cantilever laminated plate (45/0/45) of size 0.1×0.1 m is subjected to uniform pressure. The full plate is discretized into a 25×25 FE mesh. The layup sequence has been chosen to induce out-of-plane twist along with bending. It is difficult to control the coupled bending-twist deformation using isotropic actuation ($e_{31} = e_{32}$). To control the deformations in the structure, anisotropic actuation is necessary. Therefore, unidirectional piezoelectric layers ($e_{32} = 0$) with cross-ply orientation are used at the top and bottom to obtain the original undeformed configuration. These are termed piezo fiber composites (PFC), and they can be tailored to achieve desired stiffness and actuation. The PFCs permit in-plane poling. On application of the electric field in the longitudinal direction, the lamina extends in one direction and contracts in the other direction. This is unlike the conventional isotropic actuation where application of electric field in thickness direction gives rise to actuation effects in both the in-plane directions and the piezoelectric layer extends or contracts simultaneously in both the directions. In the present example we simulate this condition by removing the e_{32} effect. Although in practice the mechanical properties for the piezoelectric layer are also different in the principal material directions, here we assume that the polyvinylidenefluoride (PVDF) layer is mechanically isotropic. The initial and final designs are shown in Figs. 8a–8b. The error histories (Fig. 9) show that anisotropic actuation exercises better shape control than the isotropic actuation.

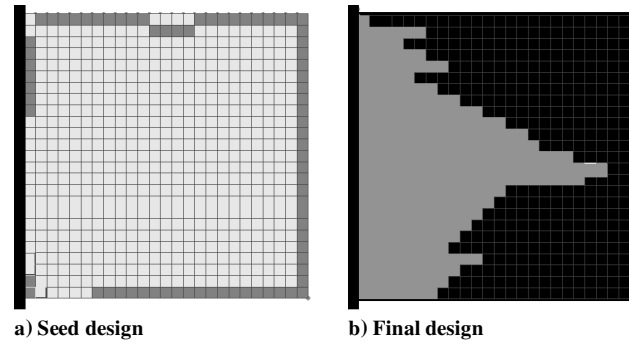

Fig. 8 Initial and final designs for anisotropic actuation (example 4).

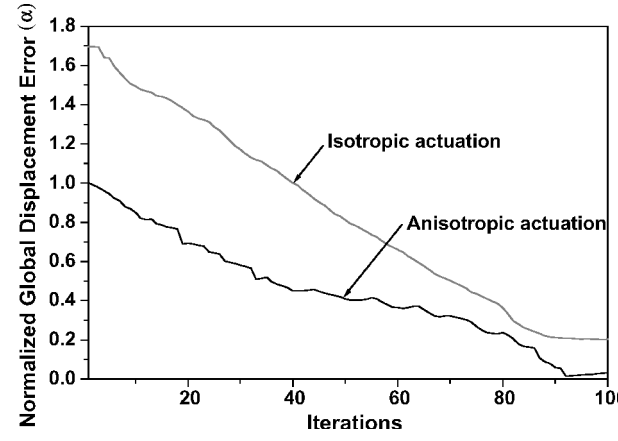

Fig. 9 Comparison of error histories for isotropic and anisotropic actuation (example 4).

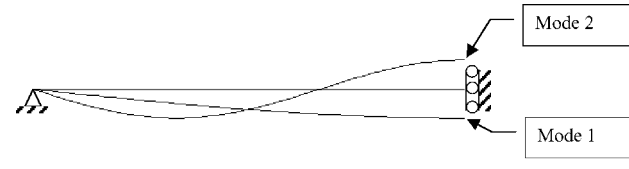

Fig. 10 First two symmetric bending modes of the plate (example 5).

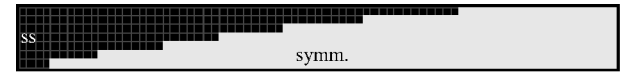

Fig. 11 Sensor design optimized for the first mode (example 5).

B. Dynamic Analysis

The applicability of the present design technique to obtain the sensor profiles corresponding to the modes that are to be observed is investigated in this section. The mode shapes are used to determine the optimum modal sensor profiles. These sensors are termed as modal sensors as they detect only those natural frequencies for which they are designed.

Example 5: A long simply supported plate. A free vibration analysis of the simply supported plate in example 2 is performed. As only a quarter of the plate is modeled, the first two symmetric modes are obtained (Fig. 10). The natural frequencies corresponding to these modes are 49.27 and 443.25 Hz. The mode shapes are then fed to the optimization routine. Figures 11 and 12 show the final sensor profiles corresponding to the first and the second modes. In Fig. 12 the

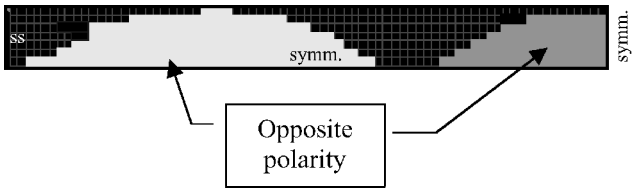

Fig. 12 Sensor design optimized for the second mode (example 5).

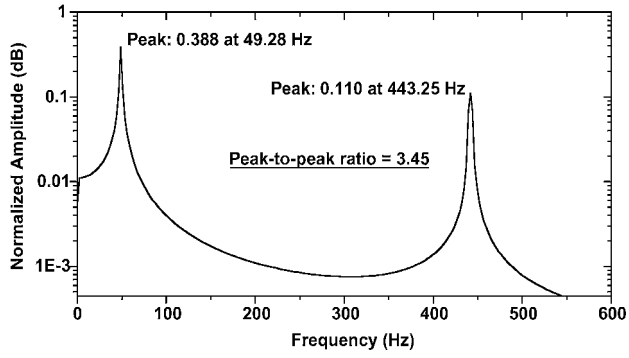

Fig. 13 Response of fully covered sensor corresponding to external excitation (example 5).

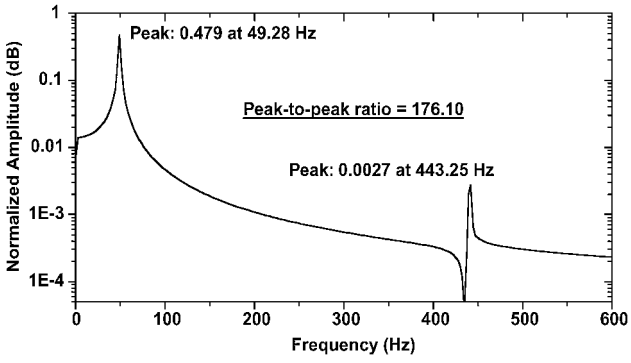

Fig. 14 Response of mode 1 sensor to external excitation (example 5).

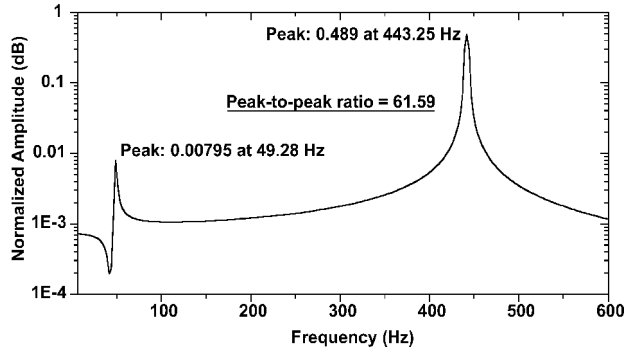

Fig. 15 Response of mode 2 sensor to external excitation (example 5).

sensors have opposite polarities because of changing curvature. To examine the efficacy of the sensor design, the structure is subjected to external excitation of nature $f = f_0(\sin\omega_1 t + \sin\omega_2 t)$, where ω_1 and ω_2 are the forcing frequencies close to the first two natural frequencies of the system. Three different sensor configurations have been examined: fully covered sensor, mode 1 sensor, and mode 2 sensor. A fast Fourier transform of the signals generated by the sensors is carried out in order to determine their frequency response. A fully covered sensor detects both the frequencies as seen from Fig. 13. The signal generated by the mode-1 sensor (Fig. 14) shows amplification of the peak corresponding to the first frequency while the second peak is diminished. Similarly, it is seen from Fig. 15 that the mode-2 sensor responds predominantly in the second mode. From the peak-to-peak ratio it can be said that the shaped sensors filter out the undesired modes successfully.

Example 6: A simply supported rectangular laminated plate. A rectangular graphite-epoxy plate (0.2×0.1 m), simply supported at all four edges, is made up of three layers (0/90/0) and a PVDF layer at the top and at the bottom. Using symmetry, only a quarter plate is modeled with a 30×15 FE mesh, and first two symmetric modes are obtained ($f_1 = 269.93$ Hz and $f_2 = 1214.76$ Hz). The sensor profiles optimized for these modes are shown for the full plate in Figs. 16 and 17. The frequency responses (Figs. 18–20)

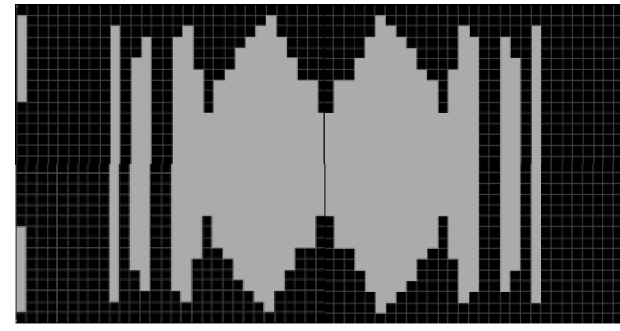

Fig. 16 Sensor design optimized for the first mode (example 6).

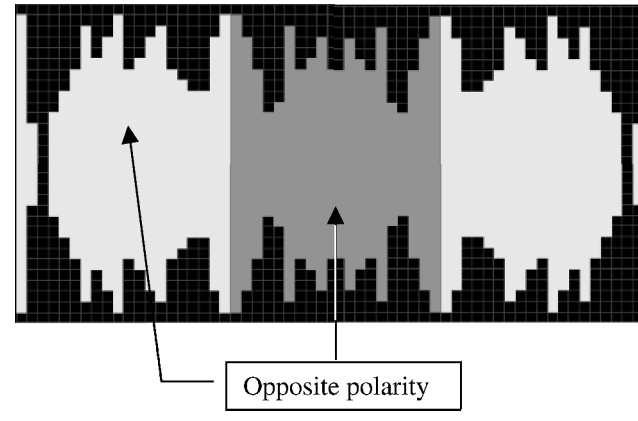

Fig. 17 Sensor design optimized for the second mode (example 6).

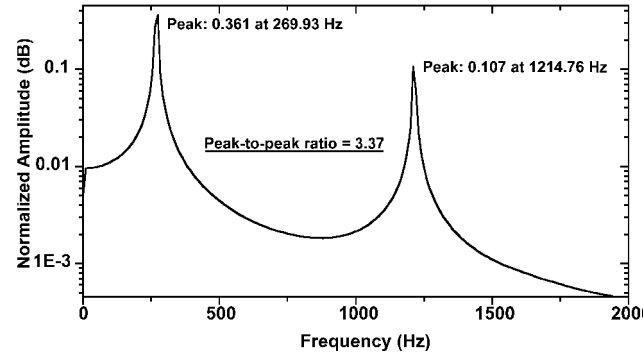

Fig. 18 Response of full sensor to external excitation (example 6).

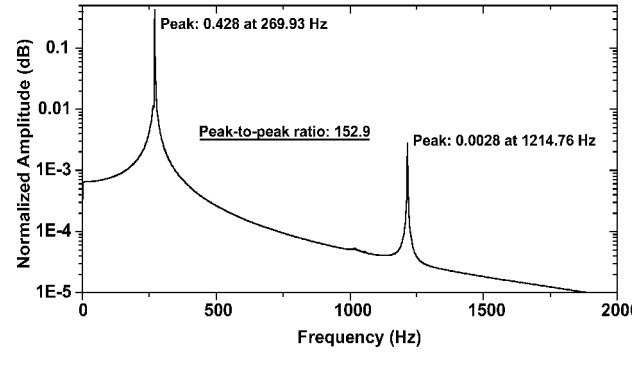

Fig. 19 Response of sensor optimized for first mode (example 6).

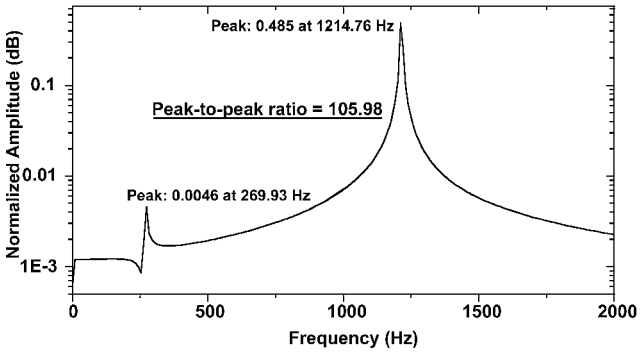

Fig. 20 Response of sensor optimized for second mode (example 6).

validate the efficacy of these two-dimensional shaped sensors in modal filtering.

VI. Conclusions

In this paper we present a gradientless iterative technique for optimal distribution of piezoelectric material to control the shape of a plate under the influence of external excitation. The design procedure has the advantage of being simple, and it can be easily integrated into the existing finite element programs. It is well suited for structures with complex geometry and boundary conditions, and it can be applied for both static as well as dynamic loads. Several numerical examples for one-dimensional and two-dimensional plate type structures have been presented. It is observed from one of the examples that controlling the plates with aspect ratios close to one, especially with free edges, is difficult using isotropic actuation. Furthermore, if there is any coupling between different deformation modes isotropic actuation does not yield a satisfactory solution. In such cases it is advisable to use directional actuation in that the piezoelectric layers are oriented such that the actuation effect can be tailored.

The present technique has also been employed in dynamic conditions to obtain sensor profiles that respond to only specific modes of interest. The efficacy of the profiles for one-dimensional as well as two-dimensional plates has been established. Because of the reciprocal relationship between a piezoelectric sensor and an actuator, the same profiles could be used as actuator profiles to excite the desired modes. These profiles can be used as spatial filters to minimize the contributions of the undesired modes in the system.

References

[1]Padula, S. L., and Kincaid, R. K., "Optimization Strategies for Sensor and Actuator Placement," NASA TM-1999-209126, April 1999.

[2]Soares, C. M. M., Soares, C. A. M., and Correia, V. M. F., "Optimal Design of Piezolaminated Structures," *Composite Structures*, Vol. 47, No. 1–4, 1999, pp. 625–634.

[3]Lim, K. B., "Disturbance Rejection Approach to Actuator and Sensor Placement," *Journal of Guidance, Control, and Dynamics*, Vol. 20, No. 1, 1997, pp. 202–204.

[4]Gawronski, W., and Lim, K. B., "Balanced Actuator and Sensor Placement for Flexible Structures," *International Journal of Control*, Vol. 65, No. 1, 1996, pp. 131–145.

[5]Clark, R. L., and Cox, D. E., "Experimental Demonstration of a Band-Limited Actutator/Sensor Selection Strategy for Structural Acoustic Control," *Journal of the Acoustical Society of America*, Vol. 106, No. 6, 1999, pp. 3407–3414.

[6]Gaudenzi, P., and Barboni, R., "Static Adjustment of Beam Deflections by Means of Induced Strain Actuators," *Smart Materials and Structures*, Vol. 8, No. 2, 1999, pp. 278–283.

[7]Barboni, R., Mannini, A., Fantini, E., and Gaudenzi, P., "Optimal Placement of PZT Actuators for the Control of Beam Dynamics," *Smart Materials and Structures*, Vol. 9, No. 1, 2000, pp. 110–120.

[8]Seeley, C. E., and Chattopadhyay, A., "The Development of an Optimization Procedure for the Design of Intelligent Structures," *Smart Materials and Structures*, Vol. 2, No. 3, 1993, pp. 135–146.

[9]Kapania, R. K., Mohan, P., and Jakubowski, A., "Control of Thermal Deformations of Spherical Mirror Segment," *Journal of Spacecraft and Rockets*, Vol. 35, No. 2, 1998, pp. 156–162.

[10]Onoda, J., and Hanawa, Y., "Actuator Placement Optimization by Genetic and Improved Simulated Annealing Algorithms," *AIAA Journal*, Vol. 31, No. 6, 1993, pp. 1167–1169.

[11]Zhang, H., Lennox, B., Goulding, P., and Leung, A., "A Float-Encoded Genetic Algorithm Technique for Integrated Optimization of Piezoelectric Actuator and Sensor Placement and Feedback Gains," *Smart Materials and Structures*, Vol. 9, No. 4, 2000, pp. 552–557.

[12]Kang, Y. K., Park, H. C., and Agrawal, B., "Optimization of Piezoceramic Sensor/Actuator Placement for Vibration Control of Laminated Plates," *AIAA Journal*, Vol. 36, No. 9, pp. 1763–1765.

[13]Lin, C. C., and Hsu, C. Y., "Static Shape Control of Smart Beam Plates Laminated with Sine Sensors and Actuators," *Smart Materials and Structures*, Vol. 8, No. 5, 1999, pp. 519–530.

[14]Agrawal, B. N., and Treanor, K. E., "Shape Control of a Beam Using Piezoelectric Actuators," *Smart Materials and Structures*, Vol. 8, No. 6, 1999, pp. 729–740.

[15]Lee, C. K., and Moon, F. C., "Modal Sensors/Actuators," *Transactions of ASME*, Vol. 57, 1990, pp. 434–441.

[16]Collins, S. A., Miller, D. W., and Von Flotow, A. H., "Distributed Sensors as Spatial Filters in Active Structural Control," *Journal of Sound and Vibration*, Vol. 173, No. 4, 1994, pp. 471–501.

[17]Friswell, M. I., "On the Design of Modal Actuators and Sensors," *Journal of Sound and Vibration*, Vol. 241, No. 3, 2001, pp. 361–372.

[18]Gaudenzi, P., Enrico, F., Koumousis, V., and Gantes, C., "Genetic Algorithm Optimization for the Active Control of a Beam by Means of PZT Actuators," *Journal of Intelligent Materials Systems and Structures*, Vol. 9, No. 4, 1998, pp. 291–300.

[19]Ryou, J. K., Park, K. Y., Kim, S. J., "Electrode Pattern Design of Piezoelectric Sensors and Actuators Using Genetic Algorithms," *AIAA Journal*, Vol. 36, No. 2, 1998, pp. 227–233.

[20]Mukherjee, A., and Joshi, S. P., "Design of Actuator Profiles for Minimum Power Consumption," *Smart Materials and Structures*, Vol. 10, No. 2, 2001, pp. 305–313.

[21]Clark, R. L., and Burke, S. E., "Practical Limitations in Achieving Shaped Modal Sensors with Induced Strain Materials," *Journal of Vibration and Acoustics*, Vol. 118, No. 4, 1996, pp. 668–675.

K. N. Shivakumar
Associate Editor